A general framework of chlorine decay modeling at a pilot-scale water distribution system

Hyunjun Kim, Jayong Koo and Sanghyun Kim

ABSTRACT

Understanding the variation of chlorine concentrations in water distribution systems is important for determining the schedule of rechlorination. Maintaining an appropriate chlorine concentration in domestic tap water and a sustainable residual chlorine in water distribution systems is an important commitment to ensure high drinking water quality. A generic modeling framework is proposed to amalgamate most widely used existing chlorine decay models. This framework gives rise to 14 distinct model structures. A pilot-scale water distribution system was designed and fabricated to investigate the performance of the proposed modeling framework. A hybrid calibration algorithm, obtained using a combination of the genetic algorithm and the particle swarm optimization, was introduced to rigorously calibrate the parameters of the various models. The adequacy of the performance of the various models was evaluated using both the Akaike information criterion and the Bayesian information criterion. A reliable relationship between the Reynolds numbers and the model parameters was obtained for the relatively simple model structure. The parameter spaces of several chlorine decay models can be configured, and equations of parameters for corresponding flow condition can be delineated. The generic model robustly predicted the chlorine concentration when the Reynolds numbers were between 15,000 and 40,000.

Key words | chlorine decay model, hydraulic condition, water distribution system

Hyunjun Kim
Sanghyun Kim (corresponding author)
Department of Environmental Engineering,
College of Engineering,
Pusan National University Busandaekak-ro 63beon-gil,
Geumjeong-gu,
Busan 609-735,
Republic of Korea
E-mail: *kimsangh@pusan.ac.kr*

Jayong Koo
Department of Environmental Engineering,
University of Seoul,
Jennongdong,
Seoul,
Republic of Korea

INTRODUCTION

Chlorine is primarily used in water treatment processes as a disinfectant (Galal-Gorchev 1996). Chlorine compounds are also widely used to prevent the spread of waterborne diseases through water distribution systems, and a sustainable chorine concentration is a critical criterion for providing safe drinking water. The presence of residual chlorine not only prevents the potential regrowth of microorganisms in water distribution systems but also provides subsidiary protection against pathogen intrusions (Mohammad *et al.* 2003). The residual chlorine concentration in water distribution systems decreases as the water travels along the distribution networks due to reactions within the bulk water and with the pipe wall (Hallam *et al.* 2003; Digiano & Zhang 2005; Mutoti *et al.* 2007; Yeh *et al.* 2008; Courtis *et al.* 2009). In the bulk water, free chlorine is mainly consumed by reactions with natural organic matter and other reacting substances. The consumption of residual chlorine at the pipe wall is mainly associated with various reactions at the attached biofilm and the corrosion surface of the pipe wall.

Many studies have been conducted to identify the relationships between the chlorine decay coefficients and influencing factors such as water temperature, initial disinfectant concentration, total organic carbon (TOC), and the amount of rechlorination (Hua *et al.* 1999; Powell *et al.* 2000; Hallam *et al.* 2003; Menaia *et al.* 2003; Courtis *et al.* 2009). Several studies have focused on factors affecting chlorine concentration to wall decay, such as pipe material, flow velocity, water quality, and the service age (Hallam *et al.* 2002; Digiano & Zhang 2005; Al-Jasser 2007; Ramos *et al.* 2010). Several studies have been performed in the modeling for disinfection by-products formation using both empirical and kinetic models (Sohn

doi: 10.2166/aqua.2014.039

et al. 2004; Di Cristo et al. 2013, 2014). However, the implementation of these influences to a model structure has not been attempted due to non-uniform and unsteady conditions in real systems.

The structure of chlorine decay models varies based on process representation and complexity (Haas & Karra 1984). Factors influencing chlorine residual have been explored in a few distinct models associated with different experimental conditions, which can result in inconsistent interpretation of the contribution of various parameters to the behavior of chlorine decay (Powell et al. 2000; Al-Jasser 2007; Mutoti et al. 2007). An experimental study with nine different chlorine models showed the potential of parameter delineation under various hydraulic conditions (Kim et al. 2014). However, a generic modeling framework is required to substantially address the differences in the structure of these models. A robust calibration scheme also seems to be required to identify the global optimum for parameter identification in the highly nonlinear space. The selection of an optimum model structure is another important issue. We have considered both the goodness of fit between observation and modeling and parsimony of parameter to determine the feasibility of applying the optimum model structure. Furthermore, we explore the effect of hydraulic conditions on chlorine decay for a stainless steel pipe system while also considering the feasibility of applying these results in experimental practice. A pilot-scale experimental pipeline system was fabricated to investigate the temporal variation in chlorine concentration. Chlorine measurements were carried out to evaluate the performance of various decay model structures.

Based on experimental operations under various hydraulic conditions, this paper highlights the following issues related to chlorine modeling in water distribution systems. First, we propose a comprehensive modeling framework to effectively evaluate the modeling efficiency of most existing chlorine decay models. A generic configuration for chlorine modeling can be obtained through an extensive exploration of model parameters under various hydraulic conditions. Second, a hybrid calibration scheme based on evolutionary computation was introduced and incorporated into the models for parameter configuration of the generic chlorine decay models. The genetic algorithm (GA) and the particle swarm optimization (PSO) are combined into a hybrid parameter optimization scheme for robust calibration of several parameter bounds (Kennedy & Eberhart 1995; Carroll 2002). Third, the impact of flow velocity condition on wall shear stress was also investigated, and the corresponding model parameter space for the Reynolds number was identified. The hydrometric environment can be implemented using parameter delineation for chlorine concentration prediction in a water distribution system. Fourth, widely accepted model selection criteria such as the Akaike information criterion (AIC) and the Bayesian information criterion (BIC) were introduced and implemented to support decision-making in the selection of models (Akaike 1974; Burnham & Anderson 2002).

MATERIALS AND METHODS

A pilot-scale experimental pipeline system

A pilot-scale experimental pipeline system was fabricated to perform experiments. As shown in Figure 1, this pipeline system comprised a closed-loop pipe, two water storage tanks, and three pumps in parallel pipes.

This pipeline system was 125 m long with a closed loop. The upstream loop began at the upstream reservoir and had a length of 65 m, while the downstream loop was stacked above the upstream loop and had a length of 60 m. Two storage tanks were used, one as a pressurized tank at the downstream boundary and the other as an upstream reservoir. The height, diameter, and storage volume of the upstream storage tank were 2 m, 0.65 m, and 660 L, respectively, whereas these values were 1.22 m, 0.98 m, and 1,000 L, respectively, for the pressurized tank. Three pumps were installed between the reservoir tank and the pressurized tank. These pumps can produce flow velocities of 0.75, 1.5, and 2.0 m/s, which generate flow conditions with Reynolds numbers between 15,000 and 400,000 throughout the system. Flow control valves were installed ahead of and behind each pump to modulate the flow velocity in the pipeline system. The pipe had an inner diameter of 0.02 m and a mean wall thickness of 0.003 m. The pipe material was stainless steel, with an elastic modulus of 190 GPa. The potential effects from biofilm

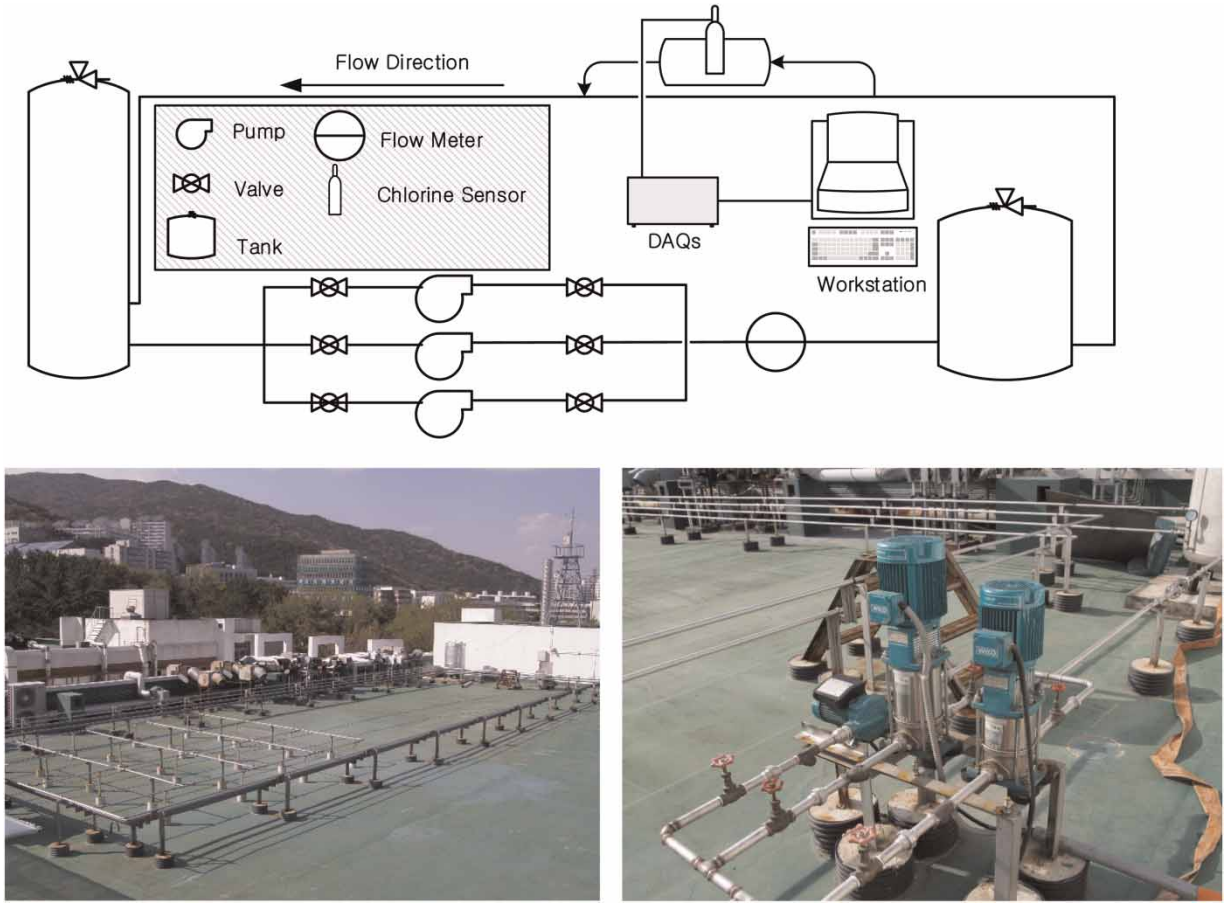

Figure 1 | Schematic and pictures of the pilot-scale experimental pipe system.

generation were minimized by cleaning the pipeline system using detergent prior to all experimental work. Mean and standard deviation of temperature during experiments were 16.3 and 1.0 °C, respectively.

Considering water disinfection in Busan Water Authority, sodium hypochlorite (NaOCl) was used for chlorine compound in experimental practices. The chlorine concentration was measured using a sampler located 33 m from the upstream reservoir. The chlorine sensor had a measurement range of 0.02–2 ppm, with an accuracy of ±0.02 ppm (Prominent Inc.). The system measured the chlorine concentration at a sampling rate of 1 Hz. The current signal (mA) from the residual chlorine sensor (4–20 mA) was sent to a data acquisition system (DAQ), and converted into a corresponding chlorine concentration (ppm) through calibration. The calibrated data were filtered using a moving average operator with a 270 sample time interval to minimize any undesirable noise fluctuation. Figure 2 shows a schematic of the DAQs used in this study. The pipeline system was filled with water from the public supply network. During the study period, the mean, maximum, and minimum of the chemical oxygen demand measurements in the public water supply system were 0.93, 1, and 0.9 mg/L, respectively. Initial chlorine concentrations ranged between 0.2 and 0.25 mg/L. The pipeline system circulated the water for 30 minutes to ensure that the initial chlorine concentration satisfied the temporally steady and spatially uniform conditions. Based on several Reynolds numbers, experiments were conducted under consistent pump and control valve conditions for 4–7 days to obtain a time series of chlorine concentration until the chlorine concentration was reduced to less than 10% of its initial concentration.

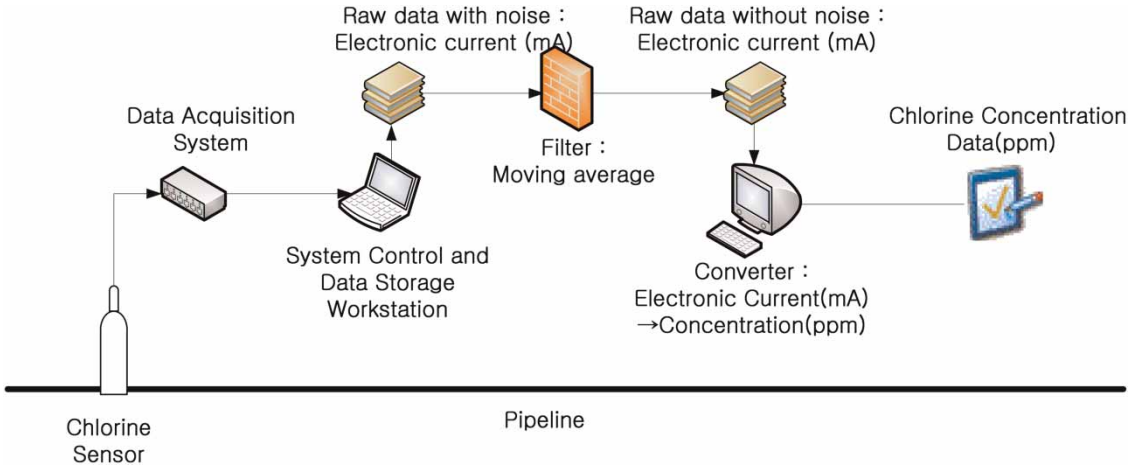

Figure 2 | Schematic of the data acquisition system for chlorine concentration.

The generic model for chlorine concentration decay

Many studies have investigated the fate of the residual chlorine concentration in water distribution systems. Table 1 lists most widely existing models that have been used to describe the decay behavior of chlorine in water systems (Haas & Karra 1984; Hua *et al*. 1999; Hallam *et al*. 2002, 2003; Vieira *et al*. 2004; Mutoti *et al*. 2007; Ramos *et al*. 2010). The 1st order model in Table 1 has been the most widely used model for the prediction of chlorine concentrations. The *n*th model was developed to improve the initial decay behavior of chlorine based on the assumption that the order *n* can describe a faster decaying rate. Limited models have been developed to express the idea that the chlorine decay is limited to a designated degree, and the redundant chlorine concentration over residual reactant has been successively described (Powell *et al*. 2000). Two distinct reactions of chlorine concentrations have been described by the parallel 1st order model, which is composed of three parameters: the fast and slow decay coefficients (k_{fast}, k_{slow}) and the weighting between the two reactions (w).

In order to compile widely used existing modeling approaches into a generic expression, a comprehensive modeling framework is introduced in this study based on the assumption that the chlorine decay can be controlled by one or multiple mechanisms and that all reactions with a simultaneous initiation are independent of each other. If the number of reactants to chlorine decay is m, then the time rate of chlorine concentration can be generalized as follows:

$$\frac{dC}{dt} = \frac{d}{dt}\left(\sum_{i=1}^{m} C_i\right) \tag{1}$$

where C_i is the partial concentration.

The reaction of the partial concentration can be expressed as follows:

$$\frac{dC_i}{dt} = -k_i(C_i - C_i^*)^{n_i} \tag{2}$$

where k_i is the decay coefficient for the ith reaction and n_i is the order of the corresponding reaction.

Initial concentration of the corresponding partial concentration can be defined as follows:

$$C_{i,0} = w_i C_0 \tag{3}$$

where w_i is the weighting for the ith reaction and $\sum_{i=1}^{m} w_i = 1$.

Table 1 illustrates the fact that most of the existing chlorine decay models can be expressed in Equations (1), (2), and (3) using combinations of the parameters m, n_i, and C_i^*. If the number of reactants is greater than two, extensive developments for more complicated models are feasible, as presented in Table 2.

Table 1 | The generic model for existing chlorine decay models

Model parameter							
m	**n_i**	**C^***		**Chlorine decay equation**	**Title**	**Calibration parameter**	**References**
1	1	0	$\frac{dC}{dt} = -kC$	$C = C_0 \exp(-kt)$	1st order	k	Mutoti *et al.* (2007), Haas & Karra (1984), Hallam *et al.* (2002, 2003), Hua *et al.* (1999), Vieira *et al.* (2004), Ramos *et al.* (2010)
1	>1	0	$\frac{dC}{dt} = -kC^n$	$C = \left(kt(n-1) + \left(\frac{1}{C_0}\right)^{(n-1)}\right)^{-\frac{1}{n-1}}$	nth order	k, n	Haas & Karra (1984), Vieira *et al.* (2004), Ramos *et al.* (2010)
1	1	≥ 0	$\frac{dC}{dt} = -k(C - C^*)$	$C = C_* + (C_0 - C_*)\exp(-kt)$	Limited 1st order	k, C^*	Haas & Karra (1984), Vieira *et al.* (2004), Ramos *et al.* (2010)
1	>1	≥ 0	$\frac{dC}{dt} = -k(C - C^*)^n$	$C = C_* + \left(kt(n-1) + \left(\frac{1}{C_0 - C_*}\right)^{(n-1)}\right)^{-\frac{1}{n-1}}$	Limited nth order	k, n, C^*	Haas & Karra (1984)
2	1	0	$\frac{dC}{dt} = \sum_{i=1}^{2}\frac{dC_i}{dt} = \frac{dC_1}{dt} + \frac{dC_2}{dt}$ $\frac{dC_1}{dt} = -k_1C_1$ $\frac{dC_2}{dt} = -k_2C_2$	$C = C_* + (w)\exp(-k_1t) + (1-w)\exp(-k_2t)$	Parallel 1st order	k_1, k_2, w	Haas & Karra (1984), Vieira *et al.* (2004), Ramos *et al.* (2010)

Table 2 | Generic models with extensive reactions

Model parameter						
m	**n_1**	**n_2**	**C^***	**Chlorine decay equation**		**Calibration parameters**
2	1	1	≥ 0	$\frac{dC}{dt} = \sum_{i=1}^{2} \frac{dC_i}{dt} = \frac{dC_1}{dt} + \frac{dC_2}{dt}$ $\frac{dC_1}{dt} = -k_1 C_1$ $\frac{dC_2}{dt} = -k_2 C_2$	$C = C_* + (w)(C_0 - C_*)\exp(-k_1 t) + (1-w)(C_0 - C_*)\exp(-k_2 t)$	k_1, k_2, C^*, w
2	1	≥ 1	≥ 0	$\frac{dC}{dt} = \sum_{i=1}^{2} \frac{dC_i}{dt} = \frac{dC_1}{dt} + \frac{dC_2}{dt}$ $\frac{dC_1}{dt} = -k_1 C_1$ $\frac{dC_2}{dt} = -k_2 C_2^{n_2}$	$C = C_* + (w)(C_0 - C_*)\exp(-k_1 t) + \left(k_2 t(n_2 - 1) + \left(\frac{1}{(1-w)(C_0 - C_*)}\right)^{(n_2 - 1)}\right)^{-\frac{1}{n_2 - 1}}$	k_1, k_2, n_2, C^*, w
2	≥ 1	≥ 1	≥ 0	$\frac{dC}{dt} = \sum_{i=1}^{2} \frac{dC_i}{dt} = \frac{dC_1}{dt} + \frac{dC_2}{dt}$ $\frac{dC_1}{dt} = -k_1 C_1^{n_1}$ $\frac{dC_2}{dt} = -k_2 C_2^{n_2}$	$C = C_* + \left(k_1 t(n_1 - 1) + \left(\frac{1}{(w)(C_0 - C_*)}\right)^{(n_1 - 1)}\right)^{-\frac{1}{n_1 - 1}} + \left(k_2 t(n_2 - 1) + \left(\frac{1}{(1-w)(C_0 - C_*)}\right)^{(n_2 - 1)}\right)^{-\frac{1}{n_2 - 1}}$	$k_1, k_2, n_1, n_2, C^*, w$

Incorporation of a hybrid optimization scheme into the chlorine models

The number of calibration parameters of the various models varies between one and six (see Tables 1 and 2), and searching for the global optimum can be computationally difficult if a size of parameter space is large. In this study, a hybrid metaheuristic optimization engine was introduced to maximize the probability, in a convergence of parameter combinations, of arriving at values close to the global optimum. Two popular algorithms, the GA and the PSO for nonlinear problems were used (Kennedy & Eberhart 1995; Carroll 2002). While GA generates new solutions for every generation until a reliable fitness is obtained, PSO also optimizes obtaining the best solution to a problem by creating a population of candidate solutions, called particles, and moving these particles around in the search-space, according to the designated mathematical formulae over the particle's position and velocity. Each particle's movement is influenced by its local best solution and is also guided towards the best solutions in the search-space, which are updated as better solutions are found by other particles (Kennedy & Eberhart 1995). Both GA and PSO are metaheuristic approaches without any assumption of the problem being optimized and can search very large spaces of candidate solutions. Furthermore, both the GA and PSO do not use the gradient of the problem being optimized, which means the optimization problem is not necessarily to be differentiable.

Based on the selected model, both the type and the number of parameters are determined, and candidate parameters are generated. The performance of a candidate solution is evaluated using the root mean square error (RMSE) between the measurements and the modeling as follows:

$$F(C_{\text{obs}}(i), C_{\text{model}}(i, P_1, P_2, \ldots, P_n)) = \sum_{i=1}^{n} (C_{\text{obs}}(i) - C_{\text{model}}(i, P_1, P_2, \ldots, P_n))^2 \quad (4)$$

where $C_{\text{obs}}(i)$ is the chlorine concentration obtained from an experiment at time step i and $C_{\text{model}}(i, P_1, P_2, \ldots, P_n)$ is an evaluated concentration using the selected model and parameters from the optimization.

Even though both GA and PSO update the solutions using evolutionary pattern, the details of intensification and diversification processes performed to obtain better solutions vary between the two algorithms (Kachitvichyanukul 2012). While GA uses the genetic information of past generation to obtain the next generation of solutions with better fitness, the location of the best fitness particle influences all the other particle velocities and locations for faster convergence in the PSO. The mutation of GA prevents early intensification and a premature clustering of PSO is associated with faster convergence. In the consideration of both the strengths and the weaknesses of the two algorithms, a hybrid optimization scheme was designed, as illustrated in Figure 3. Using identical input data and a selected model, a better optimum can be obtained from the application of the two algorithms.

RESULTS AND DISCUSSION

Data acquisition with interpretation

In order to measure the variation in the chlorine concentration under a steady flow condition, five different flow velocity conditions were maintained for several days. Figure 4 shows the temporal decay patterns of chlorine (ppm) for the five flow velocity conditions. Several fluctuations at the local scale can be explained to have been caused by the effect of abrupt temperature variations, such as rainfall event under outdoor experimental condition, on the chlorine sensor. The periods required for the reduction of the chlorine concentration to 10% of the initial concentration were 5.5, 5.2, 4.8, 4.4, and 4.0 days for velocities of 0.73, 1.17, 1.33, 1.5, and 1.95 m/s, respectively, and the mean chlorine concentration decay rates observed were 0.032, 0.036, 0.038, 0.042, and 0.047 ppm/day, respectively, which implies that a faster velocity condition produces a steeper decay rate, as shown in Figure 4.

Considering Re numbers range wall shear stress in turbulent flow condition, the Blasius equation can be used as follows:

$$\tau = 0.00395\ \text{Re}^{-0.25} \rho_{\text{water}} v^2 \quad (5)$$

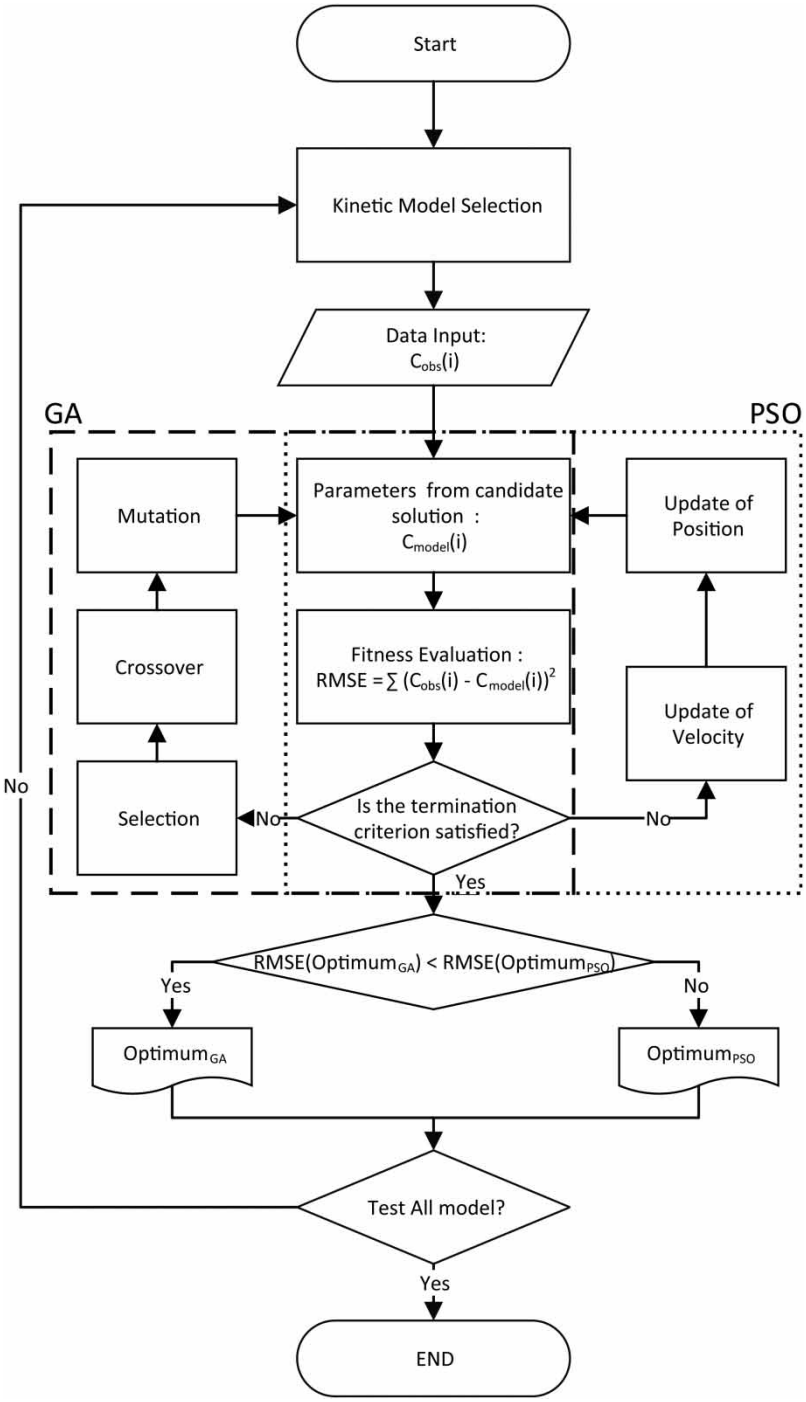

Figure 3 | Flow chart of parameter calibration using the hybrid algorithm.

where Re is the Reynolds number, ρ_{water} is the density of water, and v is the mean velocity.

The Reynolds numbers and shear stresses for different mean velocities are presented in Table 3. Biofilm density and mass are decreased as the wall shear stress is increased (Paul *et al*. 2012). The development of a wall biofilm can be reduced using high Reynolds numbers, and greater shear stresses result in higher TOC in the bulk water. The decrease in chlorine

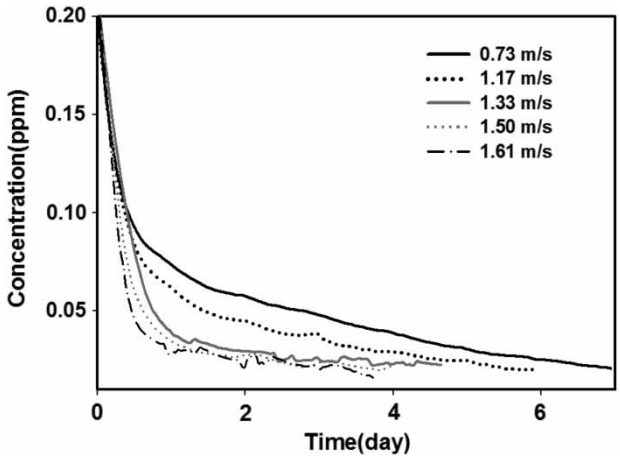

Figure 4 | Time series of chlorine concentrations under five constant flow velocities between 0.73 and 1.61 m/s.

Table 3 | Mean flow velocity, Reynolds number, and shear stress

Flow velocity (m/s)	Reynolds number	Shear stress (Pa)
0.73	14,600	1.91
1.17	23,400	4.37
1.33	26,600	5.47
1.61	32,200	7.64
1.95	39,000	10.69

concentration increases in water with higher TOC, which results in a steeper chlorine decay rate. The detachment of the wall biofilm was negligible in this study due to cleaning of the pipeline detergent prior to each experimental run. We expect chlorine concentrations to behave similarly in real-life systems, because higher shear stresses than those in this study can even deform or detach the existing biofilms as well as slow down the growth rate of the contemporary biofilm. The ranges for the bulk decay constant and the wall decay constant have previously been reported to be between 0.043 and 0.05/hour and between 0.13 and 0.22/hour, respectively (Brown *et al.* 2011). In this study, the initial development of the biofilm within a pipe of a relatively small diameter (e.g., 20 mm in this study) demands more biomass (approximately 20 times) than the biofilm in large diameter pipes used in other studies (Brown *et al.* 2011). The results of this study show that the larger the Reynolds number, the slower is the development of biofilm, which results in a steeper decay rate of the initial chlorine concentration.

Calibration of model parameters

Based on the generic model for the existing chlorine decay models (Table 1) and the generic models with extensive reactions (Table 2), 14 chlorine decay models were delineated (see Table 4) in this study. All of the chorine models in Table 4 were used for parameter calibration. Both the RMSE in Equation (4) and the coefficient of determination (R^2) were minimized between the measured chlorine time series and the calibrated chlorine concentrations using the GA and PSO optimization schemes. The population and generation numbers used to obtain solutions close to the global optimum through the GA optimization were 100 and 50, respectively. The index for the population and maximum iteration used in the PSO scheme are 100 and 50, respectively.

Table 5 presents the calibration results in terms of R^2 and the RMSE obtained using either the GA or PSO schemes. Calibrations between the GA and PSO were almost identical for the chlorine models 1–4 and 6–9 (see Table 4), which have a single parameter (k). However, those for model numbers 5 and 10–14 showed differences in calibration for either the R^2s or the RMSEs. Table 6 summarizes the calibration results using the hybrid scheme illustrated in Figure 3. Numbers of better optimization through PSO and GA were 31 and 39 out of 70 calibration practices, respectively. Calibrations for multiple parameters (e.g., model numbers 5 and 10–14) that indicated final selections through PSO and GA schemes were 13 and 17 out of 30 calibrations, respectively. No notable trend was found between the model structure and the calibration scheme. This is because the calibration spaces are too nonlinear to be characterized by metaheuristic approaches. Table 6 indicates that limited 1st order provides highest R^2s and lowest RMSEs among all model structures.

Evaluation of model performance

The performance of the generic model with extensive reactions (Table 2) showed improved fitness compared to the performance of the other existing model structures. A large number of parameters (4–6) of the models in Table 2 seem primarily responsible for better performance of the generic model than those for the other existing models in Table 1. In other words, the model structure

Table 4 | Delineated models for chlorine concentration decay

No.	Title	Governing equation	Parameters
1	1st	$C = C_0 \exp(-kt)$	k
2	2nd	$C = \left(kt + \left(\frac{1}{C_0}\right)^{(1)}\right)^{-1}$	k
3	3rd	$C = \left(2kt + \left(\frac{1}{C_0}\right)^{2}\right)^{-\frac{1}{2}}$	k
4	4th	$C = \left(3kt + \left(\frac{1}{C_0}\right)^{3}\right)^{-\frac{1}{3}}$	k
5	Nth	$C = \left((n-1)kt + \left(\frac{1}{C_0}\right)^{(n-1)}\right)^{-\frac{1}{n-1}}$	k, n
6	Limited 1st	$C = C_* + (C_0 - C_*)\exp(-kt)$	k
7	Limited 2nd	$C = C_* + \left(kt + \left(\frac{1}{C_0 - C_*}\right)\right)^{-1}$	k
8	Limited 3rd	$C = C_* + \left(2kt + \left(\frac{1}{C_0 - C_*}\right)^{2}\right)^{-\frac{1}{2}}$	k
9	Limited 4th	$C = C_* + \left(3kt + \left(\frac{1}{C_0 - C_*}\right)^{3}\right)^{-\frac{1}{3}}$	k
10	Limited nth	$C = C_* + \left((n-1)kt + \left(\frac{1}{C_0 - C_*}\right)^{(n-1)}\right)^{-\frac{1}{n-1}}$	k, n
11	Parallel 1st	$C = w_1(C_0 - C_*)\exp(-k_1 t) + (1-w_1)(C_0 - C_*)\exp(-k_2 t)$	k_1, k_2, w_1
12	Combined (1 + 1)	$C = C_* + w_1(C_0 - C_*)\exp(-k_1 t) + (1-w_1)(C_0 - C_*)\exp(-k_2 t)$	k_1, k_2, C^*, w_1
13	Combined (1 + n)	$C = C_* + w_1(C_0 - C_*)\exp(-k_1 t) + \left(k_2 t(n_2 - 1) + \left(\frac{1}{(1-w_1)(C_0 - C_*)}\right)^{(n_2-1)}\right)^{-\frac{1}{n_2-1}}$	k_1, k_2, n_2, C^*, w_1
14	Combined (n + n)	$C = C_* + \left(k_1 t(n_1 - 1) + \left(\frac{1}{w_1(C_0 - C_*)}\right)^{(n_1-1)}\right)^{-\frac{1}{n_1-1}} + \left(k_2 t(n_2 - 1) + \left(\frac{1}{(1-w_1)(C_0 - C_*)}\right)^{(n_2-1)}\right)^{-\frac{1}{n_2-1}}$	k_1, k_2, n_1, n_2, C^*, w_1

in Table 2 sufficiently addresses all combinations of the existing models depending on additional parameters, such as n_1, n_2, and w. Both the 2nd order decay model and the limited 1st order model displayed a better fitness to observational data for all the single parameter models (models 1–4 and 6–9). This is because the structure of

Table 5 | Chlorine model calibration using the hybrid scheme

Reynolds no.	17,600				23,400				26,600				32,200				38,000			
	GA		PSO		GA		PSO		GA		PSO		GA		PSO		GA		PSO	
Calibration	R^2	RMSE	R^2	RMSE	R^2	RMSE	R^2	RMSE	R^2	RMSE	R^2	RMSE	R^2	RMSE	R^2	RMSE	R^2	RMSE	R^2	RMSE
1st	0.93	0.012	0.93	0.013	0.69	0.021	0.69	0.021	0.75	0.020	0.75	0.020	0.53	0.025	0.53	0.025	0.82	0.018	0.82	.018
2nd	0.94	0.012	0.94	0.012	0.96	0.008	0.96	0.008	0.93	0.011	0.93	0.012	0.86	0.014	0.86	0.013	0.93	0.011	0.93	.011
3rd	0.82	0.020	0.82	0.020	0.94	0.009	0.94	0.009	0.85	0.015	0.85	0.015	0.85	0.014	0.85	0.014	0.82	0.017	0.82	.017
4th	0.68	0.026	0.68	0.026	0.84	0.015	0.84	0.015	0.72	0.021	0.72	0.021	0.74	0.019	0.74	0.019	0.68	0.024	0.68	.024
*N*th	0.78	0.022	0.79	0.021	0.88	0.013	0.94	0.001	0.75	0.020	0.86	0.015	0.77	0.018	0.87	0.013	0.73	0.022	0.85	.016
Limited 1st	0.93	0.014	0.93	0.014	0.91	0.011	0.91	0.011	0.96	0.008	0.96	0.008	0.87	0.013	0.87	0.013	0.97	0.008	0.97	.008
Limited 2nd	0.86	0.017	0.86	0.017	0.95	0.008	0.95	0.008	0.89	0.013	0.89	0.013	0.88	0.012	0.88	0.012	0.86	0.016	0.86	.016
Limited 3rd	0.69	0.026	0.69	0.026	0.83	0.016	0.83	0.016	0.71	0.021	0.71	0.021	0.73	0.019	0.74	0.019	0.66	0.024	0.66	.024
Limited 4th	0.54	0.032	0.54	0.032	0.71	0.021	0.71	0.021	0.55	0.026	0.55	0.026	0.58	0.024	0.58	0.024	0.50	0.029	0.50	.029
Limited *n*th	0.65	0.028	0.63	0.029	0.79	0.017	0.80	0.017	0.80	0.018	0.69	0.022	0.82	0.016	0.72	0.019	0.72	0.022	0.66	.024
Parallel 1st	0.94	0.012	0.93	0.013	0.92	0.011	0.85	0.015	0.85	0.015	0.75	0.020	0.77	0.018	0.53	0.025	0.92	0.012	0.82	.018
$1+1$	0.79	0.022	0.78	0.022	0.88	0.013	0.78	0.018	0.90	0.012	0.97	0.007	0.89	0.012	0.93	0.010	0.96	0.008	0.97	.008
$1+n$	0.89	0.016	0.97	0.009	0.95	0.008	0.97	0.007	0.96	0.008	0.93	0.011	0.89	0.012	0.88	0.013	0.91	0.013	0.93	.011
$n+n$	0.92	0.014	0.92	0.013	0.97	0.006	0.95	0.008	0.95	0.009	0.92	0.011	0.89	0.012	0.89	0.012	0.94	0.011	0.93	.011

Table 6 | Calibrations using the hybrid scheme

Reynolds no.	17,600		23,400		26,600		32,200		38,000	
Model	R^2	RMSE	R^2	RMSE	R^2	RMSE	R^2	RMSE	R^2	RMSE
1st	0.93	0.012	0.69	0.021	0.75	0.012	0.53	0.025	0.82	0.018
2nd	0.94	0.012	0.96	0.008	0.93	0.011	0.86	0.013	0.93	0.012
3rd	0.82	0.020	0.94	0.009	0.85	0.015	0.85	0.014	0.82	0.017
4th	0.68	0.026	0.84	0.015	0.72	0.021	0.74	0.019	0.68	0.024
*N*th	0.79	0.021	0.94	0.010	0.86	0.015	0.87	0.013	0.85	0.016
Limited 1st	0.93	0.012	0.91	0.011	0.96	0.008	0.87	0.013	0.97	0.008
Limited 2nd	0.86	0.017	0.95	0.008	0.89	0.013	0.88	0.012	0.86	0.016
Limited 3rd	0.69	0.026	0.83	0.016	0.71	0.021	0.74	0.019	0.66	0.024
Limited 4th	0.54	0.032	0.71	0.021	0.55	0.026	0.58	0.024	0.50	0.029
Limited *n*th	0.65	0.028	0.80	0.017	0.80	0.018	0.82	0.016	0.72	0.022
Parallel 1st	0.94	0.012	0.92	0.011	0.85	0.015	0.77	0.018	0.92	0.012
$1+1$	0.79	0.022	0.88	0.013	0.97	0.007	0.93	0.01	0.97	0.008
$1+n$	0.97	0.009	0.97	0.007	0.96	0.008	0.89	0.012	0.93	0.011
$n+n$	0.92	0.013	0.97	0.006	0.95	0.009	0.89	0.012	0.94	0.011

the 2nd order model and the limited 1st order model account for the steep initial decay trend of the chlorine concentration quite well.

With respect to model performance and the complexity of model structures, the efficiency of modeling can be evaluated in the context of the model parsimony. Both the AIC and the BIC can be used as criteria for model selection as follows (Akaike 1974; Schwarz 1978):

$$\mathrm{AIC} = m \cdot \log(\sigma^2) + 2L \tag{6}$$

Table 7 | Evaluations of AIC and BIC for all modeling conditions

Reynolds no.	17,600		23,400		26,600		32,200		38,000	
Model	AIC	BIC	AIC	BIC	AIC	BIC	AIC	BIC	AIC	BIC
1st	−378.90	−872.44	−332.73	−766.15	−338.89	−780.32	−317.82	−731.81	−349.19	−804.04
2nd	−385.68	−888.05	−422.06	−971.84	−392.40	−903.53	−371.97	−856.49	−388.45	−894.43
3rd	−337.38	−776.84	−403.19	−928.38	−361.94	−833.40	−368.25	−847.93	−349.58	−804.93
4th	−313.41	−721.66	−362.58	−834.87	−334.39	−769.95	−343.95	−791.98	−323.76	−745.49
*N*th	−329.73	−759.24	−399.50	−919.89	−362.47	−834.62	−370.13	−852.25	−355.28	−818.06
Limited 1st	−399.22	−900.21	−389.03	−895.78	−419.16	−965.15	−375.01	−863.50	−421.33	−970.15
Limited 2nd	−349.92	−805.71	−416.79	−959.69	−374.09	−861.37	−378.86	−872.36	−358.87	−826.32
Limited 3rd	−314.17	−723.41	−359.77	−828.40	−332.59	−765.81	−342.79	−789.29	−321.28	−739.78
Limited 4th	−297.11	−297.11	−335.31	−772.08	−313.51	−721.87	−322.74	−743.13	−304.18	−700.40
Limited *n*th	−306.32	−306.32	−350.57	−807.22	−346.96	−798.91	−357.09	−822.24	−328.20	−755.72
Parallel 1st	−381.25	−381.25	−387.72	−892.75	−358.29	−825.00	−344.11	−792.35	−381.35	−878.10
$1+1$	−324.46	−324.46	−367.01	−845.07	−428.37	−986.36	−392.20	−903.07	−415.86	−957.56
$1+n$	−400.90	−923.10	−405.24	−933.01	−406.39	−935.74	−371.83	−856.17	−382.12	−879.87
$n+n$	−362.21	−834.02	−426.46	−981.97	−401.07	−923.50	−372.24	−857.11	−383.23	−882.42

$$\mathrm{BIC} = m \cdot \log(\sigma^2) + \ln(m)L \quad (7)$$

where $\sigma^2 = \sum \in_i^2 / m$, ε_i is the estimated residual for a particular model, L is the number of parameters, and m is the number of data. A lower AIC or BIC represents better model efficiency and parsimony. Generally, the number of parameters, m, is highly sensitive to AIC and BIC estimations.

Table 7 presents the estimated AIC and BIC for all the models. One of the generic models with extensive reactions was observed to consistently provide the lowest AIC or BIC in all the hydraulic conditions as compared with all the other evaluations. This implies that the proposed formulation (Table 2) provides an improved framework for chlorine modeling with respective to accuracy and efficiency.

Model validation with decay parameters estimated from the hydraulic condition

The relationship between the Reynolds numbers and the decay parameters in Table 4 was analyzed applying a linear regression analysis. Table 8 summarizes the calibrated decay coefficients for several Reynolds numbers. The coefficients of determination for regressions of decay constants in the 1st to nth models and limited 1st to nth order models showed higher correlations ($R^2 \cong 0.9$) with the Reynolds numbers than those for the other complicated model structures (e.g., the parallel 1st order model and the combined model in Table 4). High R^2s in Table 8 seems strongly associated with the simple linear and limited model structures. The relatively simple model structures (see Table 4) practically explain the effect of the hydraulic condition on the modeling of the chlorine concentration. The decay coefficients for the 1st to nth models and limited 1st to nth models showed an apparent increasing tendency as the Reynolds numbers were increased in all of the models. All decay coefficients in the nth models and the limited nth models contrast with the results obtained by Menaia *et al.* (2003), which indicated that the flow velocity had no effect on the chlorine decay rate. In the Menaia *et al.* (2003) study, the experimental condition in the PVC pipes during the 8 hours of recording under a low flow velocity condition (0.56 m/s) may be responsible for the different chlorine behavior. Other studies have also shown positive correlations between the chlorine decay rate and the flow velocity (Mutoti *et al.* 2007; Ramos *et al.* 2010).

Table 8 | Linear regression equations between model parameters and Reynolds number (Re) using $y = ax + b$ and corresponding coefficients of determination (R^2) for all chlorine models

Model	y	A	b	R^2
1st linear	k	5.92×10^{-5}	−0.26	0.95
2nd linear	k	8.05×10^{-4}	−10.04	0.87
3rd linear	k	6.53×10^{-3}	−23.27	0.97
4th linear	k	9.77×10^{-2}	−646.18	0.97
nth linear	n	-1.85×10^{-5}	3.43	0.96
	k	-3.52×10^{-4}	138.91	0.47
Limited 1st	k	8.62×10^{-5}	−0.31	0.89
Limited 2nd	k	1.03×10^{-3}	−3.52	0.95
Limited 3rd	k	1.82×10^{-2}	−112.13	0.96
Limited 4th	k	4.82×10^{-1}	−5,109.3	0.97
Limited nth	n	-3.96×10^{-5}	3.90	0.64
Linear	k	-1.38×10^{-2}	657.31	0.29
Parallel 1st	w	-6.87×10^{-7}	0.35	0.00
	k_1	-9.73×10^{-5}	6.95	0.08
	k_2	5.70×10^{-5}	−0.68	0.59
$1+1$	w	-2.65×10^{-5}	0.98	0.23
	k_1	3.20×10^{-2}	−526.03	0.61
	k_2	-2.39×10^{-4}	12.66	0.05
	C^*	-1.35×10^{-6}	0.07	0.75
$1+n$	w	-2.18×10^{-6}	0.17	0.00
	k_1	-5.66×10^{-3}	696.83	0.02
	k_2	6.58×10^{-5}	45.22	0.00
	n	1.06×10^{-5}	1.73	0.07
	C^*	1.13×10^{-7}	0.00	0.01
$n+n$	w	1.56×10^{-5}	−0.16	0.89
	k_1	2.49×10^{-3}	466.33	0.05
	k_2	-6.80×10^{-4}	29.79	0.19
	n_1	-1.17×10^{-5}	3.09	0.48
	n_2	-5.20×10^{-5}	2.98	0.59
	C^*	8.21×10^{-7}	−0.01	0.63

Table 9 presents the R^2s and the RMSE values for the model validation using the parameters obtained from the regression relationships in Table 8. With respect to the model validation with the Reynolds numbers, the limited 1st order model showed the best fitness among the linear and limited model formulations, while the performance of the parallel 1st order model and the combined $(1+n)$

Table 9 | Validation of chlorine models

Reynolds no.	17,600		23,400		26,600		32,200		38,000	
Calibration	R^2	RMSE	R^2	RMSE	R^2	RMSE	R^2	RMSE	R^2	RMSE
1st	0.93	0.013	0.66	0.022	0.75	0.020	0.54	0.025	0.81	0.018
2nd	0.67	0.027	0.95	0.008	0.91	0.012	0.87	0.013	0.92	0.012
3rd	0.82	0.020	0.94	0.010	0.85	0.015	0.85	0.014	0.82	0.018
4th	0.68	0.027	0.84	0.015	0.72	0.021	0.74	0.019	0.68	0.023
*N*th	0.78	0.022	0.93	0.010	0.86	0.015	0.85	0.014	0.84	0.017
Limited 1st	0.96	0.010	0.90	0.012	0.96	0.008	0.88	0.013	0.95	0.010
Limited 2nd	0.86	0.018	0.96	0.008	0.89	0.013	0.89	0.012	0.86	0.016
Limited 3rd	0.69	0.026	0.83	0.016	0.71	0.021	0.74	0.019	0.66	0.024
Limited 4th	0.54	0.032	0.70	0.021	0.55	0.026	0.58	0.024	0.50	0.029
Limited *n*th	0.64	0.028	0.83	0.016	0.73	0.020	0.77	0.018	0.75	0.021
Parallel 1st	0.87	0.017	0.83	0.015	0.82	0.017	0.61	0.023	0.83	0.017
$1+1$	0.23	0.041	0.54	0.026	0.53	0.027	0.77	0.018	0.87	0.015
$1+n$	0.90	0.015	0.97	0.007	0.93	0.010	0.89	0.012	0.88	0.015
$n+n$	0.01	0.047	0.26	0.033	0.50	0.028	0.59	0.023	0.78	0.012

model also showed high R^2 values and low RMSEs. The high correlation of the model parameters with the flow condition does not seem to always be a necessary condition to better describe the chlorine decay for complicated model structures (e.g., combined models). The structure of a generic modeling (e.g., combined $(1+n)$ model) compensates the advantage of a simple model due to the relationship between Reynolds number and decay coefficients. Even though the relationship between the calibrated parameters and the flow condition provides an understanding of the role of hydraulics in chlorine decay behavior, the two different modeling components in the parallel 1st order model, namely, the fast and slow decay constants, and the general modeling framework (combined $(1+n)$ model), provided strengths in modeling the temporal variation in chlorine concentrations.

CONCLUSION

A general framework for chlorine decay models in water distribution systems is proposed through extension of the existing model structures. A pilot-scale pipeline system was created for an experimental evaluation of chlorine decay. Based on several distinct steady flow conditions, monitoring the water circulation in the pipeline system for 4–7 days provided a time series of variations in chlorine concentration. The structure of the generic model can be characterized into four different modeling platforms: the *n*th linear model and the limited *n*th model, a parallel 1st order model, and combined models. These modeling platforms were used to obtain 14 different chlorine model structures to test the performance of the simulation. A hybrid calibration engine using the GA and PSO was introduced for robust calibration of the model parameters under various hydraulic and model conditions. The efficiency of the model structure was evaluated using both the AIC and the BIC, and the combined model was found to be the best model in terms of model parsimony. This study also explored the relationship between the parameters of chlorine decay models and the hydraulic conditions in a water distribution system. Solid relationships were found between the decay coefficients and Reynolds numbers of the *n*th linear and the limited *n*th models. The modeling validation results showed a similar fitness as those obtained from the calibration. The proposed relationships between the model parameters and the hydraulic conditions can be used for the evaluation of several chlorine model parameters for Reynolds numbers between 15,000 and 40,000. The generic modeling framework provides a merit for robust modeling of chlorine concentration in a pipeline system. Further studies are

necessary to explore the chlorine model parameter characterization under transient pipe flow conditions.

ACKNOWLEDGEMENTS

This paper was partially supported by the Korean Ministry of Environment as 'Projects for Developing Eco-Innovation Technologies (GT-11-G-02-001-1)' and also was supported by the Basic Science Program through the National Research Foundation of Korea (NRF-2013R1A12058980).

REFERENCES

Akaike, H. 1974 A new look at the statistical model identification. *IEEE Trans. Automat. Control* **19** (6), 716–723.

Al-Jasser, A. O. 2007 Chlorine decay in drinking water transmission and distribution systems: pipe service age effects. *Water Res.* **41**, 387–396.

Brown, D., Bridgeman, J. & West, J.R. 2011 Predicting chlorine decay and THM formation in water supply systems. *Rev. Environ. Sci. Biotechnol.* **10** (1), 79–99.

Burnham, K. P. & Anderson, D. R. 2002 *Model Selection and Multimodel Inference: A Practical Information-Theoretic Approach*, 2nd edn. Springer-Verlag, New York.

Carroll, D. L. 2002 FORTRAN Genetic Algorithm (GA) Driver. http://cuaerospace.com/carroll/ga.html (5 May 2002).

Courtis, B. J., West, J. R. & Bridgeman, J. 2009 Temporal and spatial variations in bulk chlorine decay within a water supply system. *J. Environ. Eng.* **135** (3), 147–152.

Di Cristo, C., Esposito, G. & Leopardi, A. 2013 Modelling trihalomethanes formation in water supply systems. *Environ. Technol.* **34** (1), 61–70.

Di Cristo, C., Leopardi, A. & de Marinis, G. 2014 Effect of data uncertainty on trihalomethanes prediction in water supply systems using kinetic models. In: *Proceedings of the 12th International Conference on 'Computing and Control for the Water Industry – CCWI2013'*. Procedia Engineering, Elsevier, Perugia, 70, pp. 507–514.

Digiano, F. A. Z. & Zhang, W. 2005 Pipe section reactor to evaluate chlorine wall reaction. *J. Am. Water Works Assoc.* **97** (1), 74–85.

Galal-Gorchev, H. 1996 Chlorine in water disinfection. *Pure Appl. Chem.* **68** (9), 1731–1735.

Haas, C. N. & Karra, S. B. 1984 Kinetics of wastewater chlorine demand exertion. *J. Water Pollut. Control Fed.* **56** (2), 170–173.

Hallam, N. B., West, J. R., Forster, C. F., Powell, J. C. & Spencer, I. 2002 The decay of chlorine associated with the pipe wall in water distribution systems. *Water Res.* **36** (14), 3479–3488.

Hallam, N. B., Hua, F., West, J. R., Forster, C. F. & Simms, J. 2003 Bulk decay of chlorine in water distribution systems. *J. Water Res. Pl.* **129** (1), 78–81.

Hua, F., West, J. R., Barker, R. A. & Forster, C. F. 1999 Modelling of chlorine decay in municipal water supplies. *Water Res.* **33** (12), 2735–2746.

Kachitvichyanukul, V. 2012 Comparison of three evolutionary algorithms: GA, PSO, and DE. *Ind. Eng. Manage. Syst.* **11** (3), 215–223.

Kennedy, J. & Eberhart, R. 1995 Particle swarm optimization. In *Proceedings of IEEE International Conference on Neural Networks IV*, Piscataway, NJ, pp. 1942–1948.

Kim, H., Koo, J. & Kim, S. 2014 Prediction of chlorine concentration in various hydraulic conditions for a pilot scale water distribution system. In: *Proceedings of the 12th International Conference on 'Computing and Control for the Water Industry – CCWI2013'*. Procedia Engineering, Elsevier, Perugia, 70, pp. 934–942.

Menaia, J., Coelho, S. T., Lopes, A., Fonte, E. & Palma, J. 2003 Dependency of bulk chlorine decay rates on flow velocity in water distribution networks. *Water Sci. Technol. Water Supply* **3** (1–2), 209–214.

Mohammad, K., Morteza, A. & Mark, L. 2003 Potential for pathogen intrusion during pressure transients. *J. Am. Water Works Assoc.* **95** (5), 134–146.

Mutoti, G., Dietz, J. D., Arevalo, J. & Tayor, J. S. 2007 Combined chlorine dissipation: pipe material, water quality and hydraulic effects. *J. Am. Water Works Assoc.* **99** (10), 96–106.

Paul, E., Ochoa, J. C., Pechaud, Y., Liu, Y. & Line, A. 2012 Effect of shear stress and growth conditions on detachment and physical properties of biofilms. *Water Res.* **46**, 5499–5508.

Powell, J. C., Hallam, N. B., West, J. R., Forster, C. F. & Simms, J. 2000 Factors which control bulk chlorine decay rates. *Water Res.* **34** (1), 117–126.

Ramos, H., Loureiro, D., Lopes, A., Fernandes, C., Covas, D., Reis, L. F. & Cunha, M. C. 2010 Evaluation of chlorine decay in drinking water systems for different flow conditions: from theory to practice. *Water Resour. Manage.* **24** (4), 815–834.

Schwarz, G. 1978 Estimating the dimension of a model. *Ann. Stat.* **6** (2), 461–464.

Sohn, J., Amy, G., Cho, J., Lee, Y. & Yoon, Y. 2004 Disinfectant decay and disinfection by-products formation model development: chlorination and ozonation by-products. *Water Res.* **38**, 2461–2478.

Vieira, P., Coelho, S. T. & Loureiro, L. 2004 Accounting for the influence of initial chlorine concentration, TOC, iron and temperature when modelling chlorine decay in water supply. *J. Water Supply Res. Technol. – AQUA* **53**, 453–467.

Yeh, H. D., Wen, S. B., Chang, Y. C. & Lu, C. S. 2008 A new approximate solution for chlorine concentration decay in pipes. *Water Res.* **42**, 2785–2795.

First received 20 March 2014; accepted in revised form 21 October 2014. Available online 26 November 2014